DTU Library

Structural characterization of bioactive heteropolysaccharides from the medicinal fungus Inonotus obliquus (Chaga)

Wold, Christian Winther; Kjeldsen, Christian; Corthay, Alexandre; Rise, Frode; Christensen, Bjørn E.; Duus, Jens Øllgaard; Inngjerdingen, Kari Tvete

Link back to DTU Orbit

Accepted Manuscript

Title: Structural characterization of bioactive heteropolysaccharides from the medicinal fungus *Inonotus obliquus* (Chaga)

Authors: Christian Winther Wold, Christian Kjeldsen, Alexandre Corthay, Frode Rise, Bjørn E. Christensen, Jens Øllgaard Duus, Kari Tvete Inngjerdingen
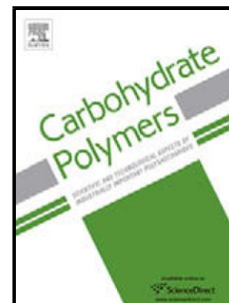
Please cite this article as: Wold CW, Kjeldsen C, Corthay A, Rise F, Christensen BE, Duus JO, Inngjerdingen KT, Structural characterization of bioactive heteropolysaccharides from the medicinal fungus *Inonotus obliquus* (Chaga), *Carbohydrate Polymers* (2010), https://doi.org/10.1016/j.carbpol.2017.12.041

Structural characterization of bioactive heteropolysaccharides from the medicinal fungus *Inonotus obliquus* (Chaga).

Christian Winther Wold[a*], Christian Kjeldsen[b], Alexandre Corthay[c], Frode Rise[e], Bjørn E. Christensen[d], Jens Øllgaard Duus[b], Kari Tvete Inngjerdingen[a]

[a] School of Pharmacy, University of Oslo, P.O. Box 1068 Blindern, N-0316 Oslo, Norway
[b] Department of Chemistry, Technical University of Denmark, DK-2800 Kgs. Lyngby, Denmark
[c] Tumor Immunology Lab, Department of Pathology, Rikshospitalet, Oslo University Hospital, P.O. Box 4950 Nydalen, NO-0424 Oslo, Norway
[d] NOBIPOL, Department of Biotechnology and Food Science, Norwegian University of Science and Technology, N-7491 Trondheim, Norway
[e] Department of Chemistry, University of Oslo, P.O. Box 1033 Blindern, N-0315 Oslo, Norway
* Corresponding author

Highlights

- Complex heteropolysaccharides were isolated from *Inonotus obliquus* sclerotia.
- The main structural motif in most fractions consisted of (1→3)- and (1→6)-β-Glc.
- A (1→6)-linked α-3-*O*-Me-Gal was found in *I. obliquus* for the first time.
- The polysaccharides displayed *in vitro* immunomodulatory effects.

Abstract

The aim of this paper was to perform a comprehensive characterization of polysaccharides isolated from the interior (IOI) and exterior (IOE) parts of the fungus *Inonotus obliquus*. Pre-extraction with DCM and MeOH, followed by water and alkali extraction and ethanol precipitation gave two water extracts and two alkali extracts. Neutral and acidic polysaccharide fractions were obtained after anion-exchange chromatography of the water extracts. The neutral polysaccharides (60-73 kDa) were heterogeneous and branched and consisted of a (1→3)-linked β-Glc backbone with (1→6)-linked kinks in the chain at approximately every fifth residue, with branches of (1→6)-linked β-Glc in addition to substantial amounts of (1→6)-linked α-Gal with 3-*O*-methylation at about every third Gal residue. The acidic polysaccharide fractions (10-31 kDa) showed similar structural motifs as the neutral fractions differing mainly by the presence of (1→4)-linked α-GalA and α-GlcA. β-Xyl, α-Man and α-Rha were also present in varying amounts in all fractions. No major structural differences between the IOI and IOE fractions were observed. An alkaline polysaccharide fraction (>450 kDa) was obtained from the IOI alkali extract, and consisted mainly of (1→3)- and (1→6)-linked β-Glc and (1→4)-linked β-Xyl. Several of the fractions showed *in vitro* immunomodulatory effect by increasing NO production in the murine macrophage and dendritic cell lines J774.A1 and D2SC/1. Most fractions managed to increase NO production only at the highest concentration tested (100 μg/ml), while the neutral

fraction IOE-WN activated potent NO production at 10 µg/ml and was considered the most promising immunomodulating fraction in this study.

1. Introduction

Inonotus obliquus (Fr.) Pilát, a rather unusual polypore fungus found in northern latitudes, has been used as an infusion in traditional medicine in Northern Europe and Russia since the 16th century against a wide range of illnesses such as tuberculosis, heart disease, cancer and stomach issues (Saar, 1991; Shikov et al., 2014). *I. obliquus* infects living, broad-leaved trees from the Betulaceae family, causing white heart rot in the tree, growing for decades while producing massive, sterile conks of sclerotia without forming fruiting bodies (Cha, Lee, Lee, & Chun, 2011; Min-Woong et al., 2008). Scientific studies have revealed many biological properties of extracts and isolated substances from *I. obliquus*, such as anti-inflammatory, anti-tumor, antioxidative and immunomodulatory properties (Chen, Huang, Cui, & Liu, 2015; Glamoclija et al., 2015; Hu et al., 2016; Lee, Lee, Song, Ha, & Hong, 2014; Ma, Chen, Dong, & Lu, 2013). Structural analysis of compounds from this fungus has revealed the presence of triterpenoids, polyphenols, melanin pigments and polysaccharides which are likely to be, at least in part, responsible for its bioactive effects (Chen et al., 2015; Hwang, Lee, & Yun, 2016; Kim et al., 2005; Youn et al., 2009; Zhao et al., 2015; Zheng et al., 2010).

Fungal polysaccharides, for example (1→3/1→6)-β-D-glucans such as lentinan from *Lentinula edodes* (Shiitake), have been associated with immunomodulatory and anti-tumor effects (Zhang, Cui, Cheung, & Wang, 2007). In Japan, lentinan is used in human cancer therapy in combination with conventional treatments such as chemotherapy to improve wellbeing and treatment outcome for patients (Ina, Kataoka, & Ando, 2013; Kapoor, 2014). Various mechanisms of action have been proposed for the anti-tumor effects of such fungal polysaccharides, with both pro- and anti-inflammatory effects being reported in the literature (Du, Lin, Bian, & Xu, 2015; Schwartz & Hadar, 2014; Zhang et al., 2007). A central mechanism of action of these compounds is their interaction with pattern recognition receptors (PRRs) on innate immune cells such as macrophages and dendritic cells (Erwig & Gow, 2016). As such, the immunological effects of the polysaccharides will depend greatly on the specific receptors involved, since different PRRs could induce different downstream effects in the cell when activated (Fraser, Stuart, & Ezekowitz, 2004). In this regard the structure and shape of the polysaccharide, including monosaccharide composition, molecular weight (M_w), branching and anomeric configuration, are important for its activity and could explain some of the conflicting reports in the scientific

literature. Further, many alleged polysaccharide extracts from medicinal fungi are shown to contain high levels of polyphenols and proteins (Wei & Van Griensven, 2008). Since some fungal compounds can activate immune cells while others can suppress the same cells a proper purification of the extracts and isolation of pure compounds are highly important to avoid additional scientific confusion (Lu et al., 2016; Wei & Van Griensven, 2008).

Although there are several reports of polysaccharides from *I. obliquus* with immunomodulatory and anti-tumor activity (Chen et al., 2015; Fan, Ding, Ai, & Deng, 2012; Kim et al., 2006; Lee et al., 2014; Rhee, Cho, Kim, Cha, & Park, 2008), satisfactory characterization of the polysaccharides including anomeric configuration and linkage analysis is lacking, and the purification methods used are often questionable. To our knowledge, the present study is the first extensive characterization of *I. obliquus* immunomodulating polysaccharides.

2. Methods

2.1 Preparation of fungal material

A fresh *Inonotus obliquus (family: Hymenochaetaceae)* specimen was harvested from a birch tree in Oslo, Norway and verified by Prof. Klaus Høiland (Dept. of Biosciences, UiO, Norway). A voucher specimen was deposited in the Pharmacognosy section, School of Pharmacy, University of Oslo, Norway. The fungal material was separated into two parts distinguished by the difference in texture and color - a brown interior part and a black exterior part – before cut into small pieces and lyophilized. The separate parts were then ground to a finely dispersed powder using an industrial blender (RAW® X1500).

2.2 Extraction of polysaccharides

In order to remove low molecular weight compounds, the fungal material (weight: 227g/131g interior/exterior) was pre-extracted in a soxhlet extractor, first with dichloromethane (DCM) for 48 h followed by methanol (MeOH) for 48 h. The remaining dried residue was then extracted first with distilled water (dH$_2$O, 100 °C, 3x, 2h) and subsequently with boiling sodium hydroxide plus sodium borodeuteride under reflux (1 M NaOH, 0.135 M NaBD$_4$, 2x, 4 h). After each extraction, the supernatant was collected after centrifugation (4000 rpm, 20 min) and concentrated under reduced pressure on a rotavapor. The extracts were then treated with pancreatin (3h, 37 °C, Sigma-Aldrich®) to degrade proteins, before ethanol precipitation (70%, 48 h, 4 °C) and centrifugation. The precipitates were finally dissolved in dH$_2$O, dialyzed (cut-off 3500 Da, 72 h, 4 °C) and lyophilized to obtain four crude polysaccharide extracts – two water-soluble extracts termed IOI-W and IOE-W (*I*nonotus *o*bliquus **I**nterior/**E**xterior **W**ater-extracted) and two alkali-soluble extracts termed IOI-A and IOE-A (*I*nonotus *o*bliquus **I**nterior/**E**xterior **A**lkali-extracted).

3

2.3 Fractionation of polysaccharides

The extraction and fractionation scheme used to obtain the purified polysaccharide fractions is presented in Fig. 1. All column chromatography experiments were carried out using an Äkta FPLC system (Pharmacia Äkta, Amersham Pharmacia Biotech, Uppsala, Sweden) with a fraction collector. All extracts and fractions were filtered through 0.45 μm Millipore filters before loaded onto the columns. The Unicorn 4.0 software (GE Healthcare, Uppsala, Sweden) was used to set-up and monitor the experiments.

2.3.1 Anion-exchange chromatography

The water-soluble crude extracts IOI-W and IOE-W (10 mg/ml) were applied to a column packed with ANX Sepharose™ 4 Fast Flow (high sub) (GE Healthcare). Neutral fractions were obtained by eluting with dH_2O (2 ml/min), while acidic fractions were obtained using a linear NaCl gradient (0–1.5 M, 2 ml/min). Fractions were collected (15 ml/tube) and carbohydrate elution profiles were monitored using the phenol-sulfuric acid method (Dubois, Gilles, Hamilton, Rebers, & Smith, 1956). The related fractions were pooled, dialyzed against dH_2O (cut-off 3500 Da) and lyophilized.

2.3.2 Size exclusion chromatography

Several fractions were subjected to gel filtration/size exclusion column chromatography (SEC) using different SEC columns. The acidic fraction from IOI-W, termed IOI-WAc (20 mg/ml), was fractionated by Hiload™ 16/60 Superdex™ 200 prep grade column (GE Healthcare), eluting with 10 mM NaCl at 0.5 ml/min and collected (2 ml/tube). The neutral fractions IOI-WN and IOE-WN (2 mg/ml) were subjected to SEC using a Superose® 6 prep grade column (GE Healthcare), eluting with 10 mM NaCl at 0.3 ml/min and collected (0.5 ml/tube).
The alkali-soluble crude extracts IOI-A and IOE-A (20 mg/ml) were subjected to SEC using a Sephacryl S-500 HR column (GE Healthcare), eluting with 0.2 M NaOH at 2 ml/min and collected (15 ml/tube). Ultimately, carbohydrate elution profiles were monitored after each experiment using the phenol-sulfuric acid method and related fractions were pooled, dialyzed and lyophilized.

4
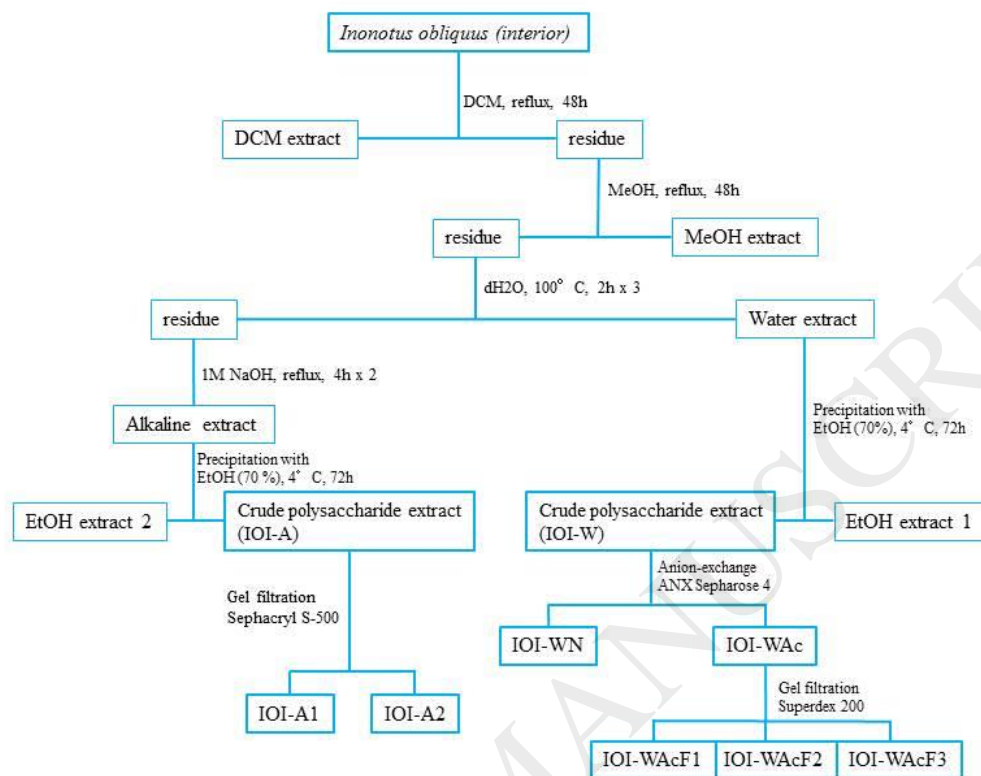
Fig. 1: Flowchart for extraction and fractionation of polysaccharides from the interior part of
Inonotus obliquus.

2.4 Molecular weight determination by SEC-MALLS

Molecular weight distributions and averages, notably the average molecular weights (M_w) of the
polysaccharides, were determined as previously described (Austarheim et al., 2012). Briefly, two
SEC columns were coupled in series, coupled to a SIL-10AF auto sampler, a LC-10ADvp pump
and a SCL-10Avp system controller (Shimadzu, Japan). Three online detectors were used, a
multi-angle laser light scattering (MALLS) Dawin Heleos-II (Wyatt, USA), a refractive index
detector (Optilab DSP, Wyatt) and a viscometer (ViscoStar, Wyatt). The column was eluted with
aqueous 0.05 M Na_2SO_4/0.01 M EDTA, pH 6 at a flow rate of 0.5 mL/min. Pullulan P8 (8 kDa)
was used for normalization of all the MALLS detectors. 100–150 μl sample solution (0.4–1.5
mg/mL) was injected. All samples were dissolved in distilled water 24 h prior to analysis, and
diluted with concentrated eluent to reach eluent concentration before injection. The samples were
run in duplicates, and M_w for each sample was calculated using the ASTRA V software (Wyatt).
A refractive index increment $(dn/dc)_\mu$ of 0.15 ml/g was used in the calculations.

5

2.5 Determination of proteins, phenolics and lipopolysaccharide in the polysaccharide fractions

The protein content of the purified polysaccharide fractions (1 mg) was determined by the Bio-Rad protein assay (Bio-Rad), based on the method of Bradford (Bradford, 1976). The standard procedure for microtiter plates was used with bovine serum albumin (BSA, Sigma) as a protein standard (30-500 μg/ml). The experiment was carried out in triplicates.

The amount of phenolic compounds in the purified polysaccharide fractions was determined using the Folin-Ciocalteu assay (Swain & Hillis, 1959). Briefly, the samples were dissolved in dH_2O (1 mg/ml) before adding the same amount of Folin-Ciocalteu's phenol reagent (1:2 in dH_2O, Merck/Kebo), mixed and left for 3 min at room temperature. 1 M Na_2CO_3 was added, before the tubes were mixed and allowed to stand for 1 h. The absorbance was measured at 750 nm. A standard curve was plotted using ferulic acid (0-50 μg/ml). The total phenolic content was determined as ferulic acid equivalents. The experiment was carried out in triplicates.

The amount of lipopolysaccharide (LPS) contamination in the purified fractions was determined by a previously described method (de Santana-Filho et al., 2012), with some modifications. Briefly, the lyophilized polysaccharide samples (5 mg) were dissolved in 3 M HCl in MeOH and incubated for 20 h at 80 °C. The solution was then partitioned between hexane (1 ml) and dH_2O (0.5 ml) three times. The hexane phase was collected, pooled and dried under a gentle N_2 stream. The samples were then acetylated at 100 °C for 1 h using a 1:1 mixture of pyridine and acetic anhydride, and thoroughly dried. Finally, acetone (70 μl) was added and the samples were analyzed by GC–MS, using the GC–MS solution software, Version 2.10 (Shimadzu Corporation). The detection limit of this assay was ~2 ng/μl.

2.6 Monosaccharide composition

The monosaccharide composition of the crude extracts and purified fractions was determined using a method originally described by Chambers and Clamp with some modifications (Chambers & Clamp, 1971; Nyman, Aachmann, Rise, Ballance, & Samuelsen, 2016). In short, the samples were subjected to methanolysis with 3 M hydrochloric acid (HCl) in anhydrous methanol (MeOH) for 24 h at 80 °C. To analyze for the presence of amino sugars, the samples were then dried using nitrogen before pyridine and acetic acid anhydride were added for 3 minutes. After drying, 0.5 M HCl in MeOH was added and the samples were incubated for 1 h at 65 °C. Trimethylsilylated (TMS) derivatives of the methyl glycosides obtained after methanolysis were analyzed by capillary gas chromatography on a Trace™ 1300 GC (Thermo Scientific™). Mannitol was used as an internal standard.

2.7 Linkage analysis by methylation/GC-MS

Glycosidic linkage analysis was performed by methylation and subsequent gas chromatography-Mass spectrometry (GC-MS) based on previously described methods (I. & Kerek, 1984; Pettolino, Walsh, Fincher, & Bacic, 2012). Briefly, polysaccharide samples (~1 mg) were first reduced using $NaBD_4$ to convert uronic acids to their corresponding neutral sugars. The polymers were then methylated with methyl iodide after dissolving in dimethylsulfoxide (DMSO) and NaOH. The per-O-methylated polysaccharides were hydrolyzed with triflouroacetic acid (TFA, 2.5 M, 4 h) and reduced with $NaBD_4$. The O-methylated alditols were acetylated by adding 1-methylimidazole and acetic anhydride and partially O-methylated alditol acetates were finally extracted with DCM and analyzed on a GCMS-QP2010 (Shimadzu Corporation) with a Restek Rxi-5MS silica column (30 m, i.d. 0.25 mm, 0.25 μm film thickness), split injection and set at a constant pressure mode. Initial flow was 1 ml/min. The injector and interface temperatures were 280°C. At the time of injection, the column temperature was 80°C, then, after 5 min, the temperature was increased with 10°C/min up to 140°C followed by 4°C/min to 210°C and then 20°C/min to 310°C, at which it was kept for 4 min. Ion source temperature was 200°C. Helium was used as the carrier gas. Spectra were analyzed using GC–MS solution software, Version 2.10 (Shimadzu Corporation).

2.8 Characterization of a (1,6)-α-3-O-methyl-galactose

2.8.1 Demethylation of monosaccharides using boron tribromide

The GC chromatograms from the monosaccharide composition analysis revealed three large peaks with unknown identity in some of the samples, which were speculated to come from a methylated hexose. To characterize this unknown compound, a method described in *Methods in Carbohydrate Chemistry, Vol II* (Whistler & Wolfrom, 1963) was used. Briefly, IOE-WN was methanolyzed as described in section 2.6, before the residue was dissolved in DCM and cooled to -80°C using a mixture of acetone and dry ice. Boron tribromide (BBr_3, -80°C) was then carefully added to the sample, and left at this temperature for 30 min to induce demethylation. The samples were then left at room temperature overnight with a drying tube with $CaCl_2$, before washed twice with MeOH, dried and analyzed by GC as described in section 2.6. Finally, the chromatogram from the demethylated sample was compared with the untreated counterpart. The standard curve from galactose was used for quantification.

2.8.2 Linkage analysis by ethylation

To establish the type of linkages and position of the methyl group, IOE-WN was subjected to ethylation and GC-MS analysis, as described in section 2.7 with one modification; ethyl iodide

was used instead of methyl iodide, which would produce unique fragmentation patterns in the GC-MS spectra.

2.9 IR spectroscopy

Infrared (IR) spectra of the purified polysaccharide fractions were obtained on a Nicolet™ FT-IR Spectrometer (Thermo Fischer Scientific). In short, dried samples (~2mm^3) were pressed onto an attenuated total reflectance (ATR) crystal using a high pressure tower to provide consistent results. The results were analyzed using the OMNIC8 software.

2.10 Nuclear magnetic resonance (NMR) spectroscopy

The water-extracted polysaccharide fractions (5-10 mg) were dissolved in 500 μl D_2O (99.9 %, Sigma). All experiments were carried out on a Bruker Avance III (799.90 MHz for 1H and 201.14 MHz for ^{13}C) equipped with a 5 mm TCI $^1H/(^{13}C, ^{15}N)$ cryoprobe using acetone as reference (2.22 ppm and 30.89 ppm for ^1H and ^{13}C, respectively). The chemical shifts were assigned using the following spectra: 1D ^1H with presaturation, 1D ^{13}C, 2D double quantum filter correlated spectroscopy (DQF-COSY), 2D total correlation spectroscopy (TOCSY) with 60 ms mixing time, 2D nuclear Overhauser effect spectroscopy (NOESY) with 200 ms mixing time, 2D ^{13}C heteronuclear single quantum coherence (HSQC) with multiplicity editing, 2D ^{13}C HSQC-[$^1H,^1H$] TOCSY (HSQC-TOSCY) with 60 ms mixing time, and 2D ^{13}C heteronuclear multi-bond correlation (HMBC) optimized for 10 Hz long range coupling constants. All spectra were recorded at 313K. Spectra were recorded using TopSpin 3.5 and processed and analyzed using the TopSpin 3.5 software (Bruker).

The alkali-extracted fraction IOI-A1 (10 mg) was dissolved in 0.1 M NaOH with D_2O (99.9%, Sigma). Experiments were carried out on a Bruker Avance III HD Ascend (800.03 MHz for ^1H and 201.17 MHz for ^{13}C) equipped with a 5 mm TCI $^1H/(^{13}C, ^{15}N)$ cryoprobe using the internal standard TMSP-$_{d4}$ 3-(trimethylsilyl)-2,2,3,3-tetradeuteropropionic acid sodium salt as reference. The chemical shifts were assigned using the following spectra: 1D ^1H with presaturation and excitation sculpting solvent suppression, 1D ^{13}C, 2D DQF-COSY, 2D TOCSY with 80 ms mixing time, 2D NOESY with 300 ms mixing time and 2D ^{13}C HSQC with multiplicity editing. Spectra were recorded at 313 K and acquired, processed and analyzed using TopSpin 3.5.

2.11 Periodate oxidation and Smith degradation

Periodate oxidation and Smith degradation of was carried out as previously described (Kamerling & Gerwig, 2007). In short, IOE-WN and IOI-WAc (15 mg) were oxidized with 0.05 M sodium periodate (3 mL) and 0.2 M acetate buffer pH 4.0 (3 mL) at 4°C in the dark with stirring for 48 h. The oxidation was terminated by addition of 1% ethylene glycol and kept for 1

h before desalting using a PD-10 column (GE Healthcare). The samples were reduced with NaBH$_4$ (60 mg) and left at room temperature overnight. The reaction mixture was neutralized to pH 7.0 with 1 M acetic acid on ice and desalted again before hydrolysis with 0.05 M TFA for 30 min at 100°C. The samples were neutralized using 1 M NaOH and analyzed and fractionated using a CarboPac™ PA100 ZOU column (Dionex, ThermoFisher) with galactose, glucose, maltotetraose and maltohexaose as standards (Sigma). Finally the fractions were collected and subjected to methanolysis and GC analysis as described in section 2.6.

2.12 Cell lines

The murine macrophage cell line J774.A1 (a gift from Anders Gammelsrud, Norwegian Veterinary Institute) and the murine dendritic cell line D2SC/1 (a gift from Francesca Granucci, University of Milan) were grown in RPMI medium with 10 % FBS, 5 % streptomycin/penicillin, 1 % NEAA and 1 % mercaptoethanol, and incubated at 37 °C, 5% CO$_2$. Prior to the experiments both cell lines were tested and found to be negative for Mycoplasma infection.

2.13 Nitric oxide assay

Nitric oxide (NO) production by activated immune cells was measured using the Griess reagent system (Promega). Briefly, J774.A1 and D2SC/1 cells were seeded at a density of 5×10^5 cells/ml in flat-bottomed 96-well plates to a total volume of 100 μl, and stimulated for 24 h with increasing concentrations of polysaccharide samples together with interferon-gamma (20 ng/ml, recombinant murine IFN-γ, Peprotech). After 24 h, the supernatant was collected and Griess reagents A and B were added to convert NO into nitrite (NO$_2^-$), which could be quantified colorimetrically using a dilution series of NaNO$_2$ as a standard curve. The absorbance was measured at 540 nm. LPS (1 μg/ml, from *E.coli 055:B5*, Sigma) and Pam3CSK4 (2 μg/ml, InvivoGen) with and without IFN-γ (20ng/ml), IFN-γ alone and untreated cells were used as controls. The nitrite value from the untreated negative control was set to zero and the value was subtracted from the other samples. The experiments were carried out in duplicates, and repeated two (D2SC/1) or three (J774.A1) times.

3. Results and discussion

3.1 Extraction and fractionation of polysaccharides

I. obliquus was separated into an interior and exterior part and extracted using a stepwise procedure with solvents of increasing polarity (Fig. 1). The extracts obtained by DCM and MeOH extraction were saved for later studies. Water- and alkali extraction, protease treatment and ethanol precipitation of the remaining fungal mass gave the four crude polysaccharide extracts, IOI-W, IOE-W, IOI-A and IOE-A. Since this procedure is a widely accepted method for

9

isolation of crude polysaccharides from plants and fungi, it was expected that the main component in these extracts was polysaccharides (Bouchard, Hofland, & Witkamp, 2007; Zhang et al., 2007). However, all four crude extracts appeared dark brown in color, indicating presence of substances other than polysaccharides. *I. obliquus* is known to contain massive amounts of melanin pigments, reported to be the main content in *I. obliquus* water extracts (Shashkina, Shashkin, & Sergeev, 2006). One study reported a 57 kDa allomelanin pigment isolated from *I. obliquus*, which could explain why the color remained in the extracts even after dialysis and ethanol precipitation (Kukulyanskaya, Kurchenko, Kurchenko, & Babitskaya, 2002). Indeed, the fractions obtained after anion-exchange chromatography of the crude water-extracts revealed that only a minor part of the extracts were polysaccharides. The crude extract IOI-W (3.2 g) gave two polysaccharide fractions - IOI-WN (80 mg) and IOI-WAc (75 mg) – which combined were responsible for 4.8 % of the total extract weight, or 0.45 % of total interior *I. obliquus* dry weight. Although most of the pigment was trapped in the ANX sepharose resin when eluting with water, some of the color came out with the acidic fractions IOI-WAc and IOE-WAc. The presence of phenolics was later detected in the acidic fractions (Table 1). Previous studies have reported fungal melanin to have a polyphenolic structure (Eisenman & Casadevall, 2012; Prados-Rosales et al., 2015), and in agreement with this phenolics were not detected in the fractions where the color was absent, such as IOI-WN. After anion-exchange chromatography, IOI-WN, IOE-WN and IOI-WAc were subjected to SEC. IOI-WAc was fractionated using Superdex 200, giving the fractions IOI-WAcF1, IOI-WAcF2 and IOI-WAcF3 in that order (Fig. S30). The other samples could not be fractionated further (Fig. S27-29).

Alkaline extraction of fungal polysaccharides has been reported to be a promising method that could increase polysaccharide yields (Huang et al., 2010). We have previously optimized a method in our lab for this extraction method by adding sodium borodeutride which could protect the reducing ends and thus prevent the polymers from degrading (see section 2.2 for details). However, the downside to alkaline extraction is that it could also cause degradation of labile side-groups in the polymer such as methyl- and acetyl groups (unpublished results). The alkali-extracted interior part yielded a relatively pure polysaccharide fraction after SEC - IOI-A1 - accounting for 12.5 % of the alkaline crude extract (~ 1 % of total dry interior weight). In contrast, the extract from the exterior part yielded only heavily pigmented fractions after SEC with low amounts of polysaccharide (IOE-A1 and IOE-A2) and these were not analyzed further in this study. The presence of melanin in the polysaccharide extracts highlights the importance of proper fractionation when isolating polysaccharides from *I. obliquus*, especially if biological assays will be conducted.

3.2 Molecular weight determination by SEC-MALLS

The weight-average molecular weights (M_w) of the polysaccharide fractions and weight average radius of gyration (R_G) values were determined by SEC-MALLS analysis (Table 1, Fig. S19-

S26). The neutral polysaccharides IOI/IOE-WN had higher M_w than the acidic ones (60/73 kDa vs 10-31 kDa), while the alkaline-extracted IOI-A1 gave the highest M_w of ~2000 kDa. However, the M_w of IOI-A1 must be interpreted with caution, since the SEC-MALLS analysis was conducted at pH 6 while IOI-A1 is poorly soluble at pH<8. An HPLC analysis of this sample was therefore carried out in addition to SEC-MALLS, dissolving IOI-A1 in 10 mM NaOH. The HPLC experiment indicated a polymer size larger than the biggest dextran standard utilized, which was 450 kDa (data not shown). IOI-WN and IOE-WAc were suggested to contain more than one type of polymer, but when using prep grade SEC it was not possible to fractionate these any further. IOI-WAc was also suggested to contain more than one polymer. In the SEC-MALLS chromatogram of IOI-WAc (Fig S21), only one main peak can be observed. However, the peak was quite broad, indicating that it could contain polymers of more than one size. This seemed to be the case, as IOI-WAc was fractionated into the three sub-fractions IOI-WAcF1-F3 by gel filtration (Fig. 1). In general, the SEC chromatograms, notably the light scattering profiles, were too irregular for conventional data analysis, making it difficult to estimate the radius of gyration (R_G) values, as well as the number-average molecular weights (M_n). Nevertheless, the R_G (weight average) ranges observed across the peaks indicated that the polymers were in some cases rather compact structures, possibly aggregates, which could explain why we could not manage to further fractionate IOI-WN and IOE-WAc by SEC. There are a few reports in the literature on molecular weight of polysaccharides from *I. obliquus*. One group found a 48.8 kDa water-soluble polysaccharide from wild *I. obliquus*, in reasonable agreement with our own data (Chen et al., 2015). Another study reported water-soluble *I. obliquus* polysaccharides with a wide range of sizes, from <10 kDa up to 1.100 kDa (Kim et al., 2005), but the use of cultivated *I. obliquus* mycelium instead of wild fungus makes it difficult to compare these results directly with our own.

3.3 Purity of the polysaccharide fractions and LPS contamination

Table 1 gives an overview of the purity of the polysaccharide fractions, showing carbohydrate content, protein content, phenolic content and LPS contamination in the fractions. The fractions had a carbohydrate content ranging from 41.9-89 %. The percentages are based on the GC analysis, using mannitol as internal standard. It should be noted that there is some uncertainty to the calculations of these percentages. The peak coming from glucose in the GC chromatogram was too big for accurate quantification, possibly leading to an underestimation of actual content of this monosaccharide, but when diluting the samples the peaks from several of the other monosaccharides became too small. However, there was a high uncertainty in these calculations. In addition, the calculation for 3-*O*-Me-Gal was based on the galactose standard curve, meaning it could have been inaccurately quantified. All fractions were essentially free from proteins, as would be expected since the extracts were treated with a protease prior to fractionation. The phenolic content was related to the presence of melanin pigments as discussed in section 3.1. The acidic fractions had a higher content of phenolics than the neutral fractions. For example, IOI-

WN did not contain any phenolics, while IOI-WAc had a phenolic content of 6.7 %. This suggests that the pigments are not covalently bound to the polysaccharides, although a possible explanation could be that the galacturonic acid (which is present in large amounts in the acidic fractions) interacts with the pigments in some way. When IOI-WAc was further fractionated with SEC, the three sub fractions IOI-WAcF1 – F3 contained 4,2 %, 5.8 % and 9.7 % phenolics, respectively, suggesting that the melanin pigments range in size from at least 10-31 kDa. The alkali extracted IOI-A1 also contained some phenolic traces, accounting for 0.4 % of total sample weight. The samples were analyzed for the presence of LPS, a constituent of the outer cell membrane in gram-negative bacteria and a common contaminant in natural products research (Lieder, Petersen, & Sigurjonsson, 2013). Only the acidic fraction IOE-WAc from the exterior part was found to contain LPS, accounting for 0.16 % of the total sample weight which is equivalent to 160 ng/ml LPS in a 1 mg/ml sample. Biological assays are often highly sensitive to LPS, and it has been reported that LPS at less than 1 ng/ml can be recognized by human immune cells (Lieder et al., 2013). This underlines the need for caution when interpreting results when using natural products in such assays, and the analysis for the presence/absence of LPS should always be carried out prior to the experiments.

Table 1: M_w, R_G, carbohydrate content, protein content (expressed as albumin), total phenolic content (expressed as ferulic acid) and LPS content in the isolated polysaccharide fractions.

Fraction	M_w (kDa)	R_G (nm)	Total carbohydrate (%)	Total protein (%)	Total phenolics (%)	LPS contamination
IOI-WN	60	57[1]	89	<0.1	<0.1	n.d.
IOI-WAc	15	<10-15[2]	69.1	<0.1	6.7	n.d.
IOI-WAcF1	28	17	81.9	<0.1	4.2	n.d.
IOI-WAcF2	14	<10-15[2]	61.2	<0.1	5.8	n.d.
IOI-WAcF3	10	<10-15[2]	58.3	<0.1	9.7	n.d.
IOE-WN	73	36	54.7	<0.1	<0.1	n.d.
IOE-WAc	31	29[1]	47.3	<0.1	2.0	0.16 %
IOI-A1	>450	n.e.	41.9	<0.1	0.4	n.d.

[1] may be grossly overestimated due to irregular light scattering data; [2] below detection limit; n.e. = not established; n.d. = not detected; Limit of detection for LPS: 2 ng/µl (de Santana-Filho et al., 2012).

3.4 Monosaccharide composition

The monosaccharide composition of the polysaccharide fractions is presented in Table 2. The most common monosaccharide in all water-soluble fractions was glucose, with galactose, mannose and xylose present in substantial amounts. The acidic fractions had high levels of galacturonic acid and increased amounts of rhamnose compared to the neutral fractions, while arabinose, fucose and glucuronic acid were present in minor amounts in all fractions. 3-*O*-methyl-galactose (3-*O*-Me-Gal) was found in varying amounts in all fractions, and the amount decreased with decreasing size of the polymer, as seen by comparing the acidic fractions IOI-WAcF1, F2 and F3 (Table 1 and 2). The alkali-extracted IOI-A1 contained mainly glucose (79.2 %) and xylose (12.1 %), with traces of mannose, fucose and N-acetylglucosamine (GlcNAc). There are a few publications on isolated and purified *I. obliquus* polysaccharides. Chen et al. isolated a polysaccharide consisting of rhamnose, arabinose, glucose and galactose in a molar ratio of 2.5:4.6:1.0:2.6 with approx. 30 % uronic acid (Chen et al., 2015), while Fan et al. isolated a polysaccharide consisting of rhamnose, mannose and glucose in ratio 1.0:2.3:1.7 with 7.5 % uronic acid (Fan et al., 2012). The high amounts of arabinose and rhamnose in these studies are in contrast to our own data. There are several possible explanations for the differences, such as isolation methods, harvest location and age of the fungus, and which part of the fungus was used. Since arabinose and rhamnose are typical plant monosaccharides (Liu, Willför, & Xu, 2015), it could also be possible that the *I. obliquus* samples were "contaminated" with birch material after harvesting, which is quite common when collecting wild-grown *I. obliquus* sclerotia. Apart from these papers, most of the studies on *I. obliquus* polysaccharides have been carried out using cultured mycelium rather than wild-grown fungi, and the results are therefore not directly comparable (Kim et al., 2006; Xu, Quan, & Shen, 2015).

Table 2: Monosaccharide composition (mol %) after methanolysis and GC of the polysaccharide fractions isolated from *I. obliquus*.

Monosaccharide	IOI-WN	IOE-WN	IOI-WAc	IOI-WAcF1	IOI-WAcF2	IOI-WAcF3	IOE-WAc	IOI-A1
Arabinose	1.4	2.0	2.1	2.3	2.3	2.4	0.9	n.d.
Rhamnose	1.3	1.3	5.1	4.8	5.4	7.7	3.4	n.d.
Fucose	1.7	2.5	1.3	1.5	1.0	0.7	0.5	2.8
Xylose	6.9	8.9	8.8	4.7	5.2	19.0	6.0	12.2
Mannose	6.8	7.2	8.2	10.8	13.4	4.8	8.4	4.0
Galactose	17.5	17.2	11.2	13.5	9.6	8.1	15.6	n.d.
Glucose	53.1	49.3	37.9	34.3	43.1	39.2	31.6	78.2
Glucuronic acid	1.0	2.1	5.1	4.4	4.0	4.4	3.1	n.d.
Galacturonic acid	1.8	1.2	15.7	17.7	13.1	12.9	24.3	n.d.
3-*O*-methyl galactose	8.7	8.3	4.6	6.0	2.9	1.1	6.2	n.d.

N-acetylglucosamine	n.d.	n.d.	n.d.	n.d.	n.d.	n.d.	n.d.	2.8
Sum %	100	100	100	100	100	100	100	100

(n.d. = not detected)

3.5 Chemical determination of (1→6)-α-*3-*O-*Me-Gal*

The results from the monosaccharide composition analysis by GC revealed three unknown peaks in the chromatogram, which based on previous discoveries in our lab was suggested to come from a methylated hexose (Fig. 2). To identify the unknown compound, IOE-WN was demethylated using BBr$_3$ and analyzed by GC after methanolysis before compared with the original GC data. The three peaks in question disappeared after demethylation, while the ratio between mannose, galactose and glucose had changed from ~1:2:7.5 to ~1:3:6, suggesting that the methylated species was a galactose. The IOE-WN fraction was ethylated and analyzed by GC-MS to find the position of the methyl group. From the linkage analysis data (Table 3) it was seen that most of the galactose was (1→6)-linked, and therefore we searched for fragments which matched this configuration, theoretically placing the methyl group in position C2, C3 or C4 to see which fragments were expected after ethylation. We located a large peak containing the fragments 132, 190, 203 and 261 m/z, which were expected if a hexose was methylated at C3. Ultimately, this finding was verified by NMR spectroscopy including anomeric configuration (Fig. 3, Table 4), suggesting presence of (1→6)-α-3-*O*-Me-Gal residues in most fractions. The present study is the first to report this uncommon monosaccharide in *I. obliquus.* There are some papers describing (1→6)-α-3-*O*-Me-Gal from other fungi, such as species from the genera *Phellinus* and *Pleurotus* (Carbonero et al., 2008; Yang et al., 2007). With the presence of this residue in *Inonotus* as well, it seems that extensive 3-*O*-methylation of galactose is more common in polypore fungi than previously thought, although the biological role of such methylation is still largely unknown (Staudacher, 2012).
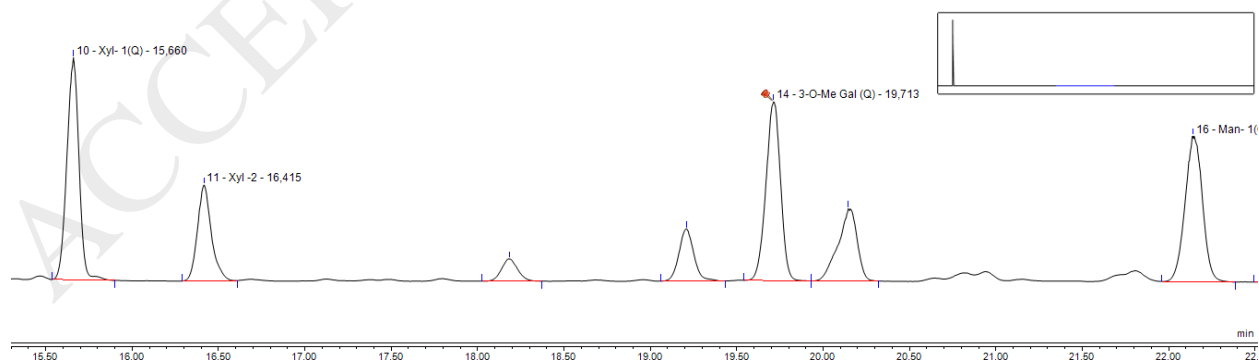

Fig. 2: The three chromatographic peaks (19-20.50 min) from 3-*O*-Me-Gal after methanolysis and GC analysis of IOE-WN, located between the peaks from xylose (15.5-16.5 min) and mannose (22 min).

14

3.6 Linkage analysis by methylation/GC-MS

To reveal how the different monosaccharides were linked, the methylated alditol acetates of the monosaccharides were analyzed by GC-MS, as seen in Table 3. The results are presented as total mol% of each sub-species based on the percentage of each monosaccharide initially found by GC analysis after methanolysis (Table 2). The most common glucose species in the water-extracted fractions were (1→3)-linked Glc and (1→6)-linked Glc. There were also substantial amounts of terminal (non-reducing) Glc (T-Glc) and (1→3, 6)-linked Glc, indicating a highly branched structure of the polysaccharides. The presence of (1→2, 3)-linked Glc (~1%) and (1→2, 3, 6)-linked Glc (~1%) suggest that glucose could be substituted at position C2 by arabinose, fucose, xylose and glucuronic acid, which were all present in minor amounts and were mostly of terminal origin. Galactose was the second most common monosaccharide, being almost exclusively (1→6)-linked, with small amounts of T-Gal and (1→2, 6)-linked Gal indicating that also galactose was substituted at C2. The percentage of the different galactose species found from GC-MS is a combination of native and methylated galactose, since these two types would appear identical after methylation of the samples, except for (1→3) - and (1→3, 6)-linked Gal which only could come from native galactose. Mannose was mostly (1→2)- and (1→3)-linked, with some T-Man as well. The acidic fractions had substantial amounts of (1→4)-linked GalA, which was virtually absent in the neutral fractions IOI-WN and IOE-WN.

The presence of (1→4)-linked GalA, (1→2)- and (1→2, 4)-linked Rha, as well as some (1→3)-linked Gal and T-Ara indicates that a part of the polysaccharides had a pectin-like structure (Yapo, 2011). It could be that some birch material was mixed with the fungal material prior to extraction and fractionation. If this were true, the traces should only be prominent in the fractions isolated from the interior part of the fungus, since this part is in direct contact with the birch. Since fractions isolated from both the interior and exterior parts contained the pectin-resembling linkages, it is likely that there exists some other explanation for the linkages observed.

Table 3: Glycosidic linkages (mol %) in the polysaccharide fractions isolated from *I. obliquus* detected by GC-MS analysis of methylated alditol acetates.

Linkage	IOI-WN	IOE-WN	IOI-WAc	IOI-WAcF1	IOI-WAcF2	IOI-WAcF3	IOE-WAc	IOI-A1
Ara								
T	1.4	2	2.1	2.3	2.3	2.4	Trace	n.d.
Rha								
T	n.d.	Trace	Trace	Trace	2.3	n.d.	1.4	n.d.
1,2	Trace	Trace	2.1	2.1	1.1	5	Trace	n.d.
1,3	Trace	Trace	n.d.	n.d.	n.d.	n.d.	n.d.	n.d.
1,2,4	n.d.	Trace	2.1	2	2	2.7	1	n.d.

15

Fuc								
T	1.7	2.5	1.3	1.5	1	Trace	Trace	1.9
Xyl								
T	3.1	4.7	5.3	3.3	3.5	3.7	2.6	2.8
1,4	3.8	4.2	3.5	1.4	1.7	16.3	3.4	9.4
Man								
T	1.6	1.4	1.8	1	1.8	2.5	2.6	n.d.
1,2	2.4	2.4	3.2	5.3	1.8	n.d.	2.4	n.d.
1,3	2.8	3.4	3.2	4.5	9.8	2.3	3.4	3.5
Gal								
T	Trace	2.8	2.2	1.3	3.6	6.1	1.1	n.d.
1,4	Trace	n.d.	1.2	Trace	1.4	n.d.	Trace	n.d.
1,3	Trace	1.1	Trace	Trace	Trace	n.d.	Trace	n.d.
1,6	22.1	17.9	9.4	14.4	6.1	3.1	17.2	n.d.
1,2,6	2.2	2	1.2	1.8	n.d.	n.d.	2.7	n.d.
1,3,6	Trace	1.1	Trace	1.3	Trace	n.d.	Trace	n.d.
Glc								
T	9.5	9.7	7.1	6.9	9.7	7.9	4.8	7.8
1,3	19	17.2	12.3	12	12.8	22.1	10.1	55.6
1,4	1.7	3.1	3.2	1.6	7	Trace	2	n.d.
1,6	16.2	12.8	9.6	8.2	10.3	6.1	9.1	3.2
1,3,4	Trace	Trace	Trace	Trace	n.d.	n.d.	Trace	2.6
1,2,3	Trace	1.3	Trace	1	n.d.	n.d.	1.3	2.5
1,3,6	5.3	5.1	4.6	3.8	2.9	2.1	3.3	5.9
1,4,6	Trace	Trace	Trace	Trace	Trace	n.d.	Trace	n.d.
1,2,3,6	1	Trace	1.1	Trace	Trace	Trace	1.0	Trace
GlcA								
T	Trace	1.2	1.7	1	n.d.	n.d.	2.5	n.d.
1,4	Trace	trace	3.4	3.4	4	4.4	Trace	n.d.
GalA								
T	Trace	Trace	3.8	1.1	n.d.	1.4	3.2	n.d.
1,4	n.d.	Trace	10.2	11.2	13.1	11.5	16.5	n.d.
1,3,4	1.3	Trace	1.6	5.4	n.d.	n.d.	4.6	n.d.

(n.d. = not detected; trace = less than 1 %; T = terminal, non-reducing end)

3.7 IR spectroscopy

The polysaccharide fractions were analyzed by IR spectroscopy. There were several bands in the IR spectra that could be assigned to structural motifs from carbohydrates. There was a strong, but broad band at 3360 cm^{-1} coming from –OH groups, and several bands around 900-1050 cm^{-1} that probably came from (C-O-C) in glycosidic linkages of various configurations. The bands from C-O-C will usually shift slightly depending on type of linkage (α, β, 1→6 vs 1→3 etc.) and it was therefore expected that this area was crowded with signals, as observed in the spectra (Wiercigroch et al., 2017). In addition, a band with strong intensity could be observed at 1650 cm^{-1} in the acidic fractions, probably from a C=O in a carboxylic group coming from the uronic acids.

3.8 NMR spectroscopy

The NMR data were interpreted by comparing and matching chemical shift values from the 1D spectra ^{1}H and ^{13}C, and 2D spectra DQF-COSY, TOCSY, NOESY, HSQC, HSQC-TOSCY and HMBC. It was possible to deduce the monosaccharide structure for many of the major signals, including possible linkages. The polysaccharide fractions were analyzed separately, and differences between them were deduced by comparing the different NMR spectra and by comparison with GC- and GC-MS data. CASPER predictions and reference values from the literature were also used to assign the chemical shift values (Agrawal, 1992; Duus, Gotfredsen, & Bock, 2000; Jansson, Stenutz, & Widmalm, 2006; Lundborg & Widmalm, 2011). In general, the signals belonging to the different monosaccharide species were assigned using the following procedure: First, an anomeric (H1) ^{1}H-^{1}H signal was located in a DQF-COSY spectrum. The H1 signal was then correlated with the H2 signal in the same spin system, and it was attempted to find further correlations to H3 and so on, using DQF-COSY and TOCSY. If the rest of the spin system could not be determined this way, HSQC-TOCSY, HMBC and NOESY spectra were used to find the last ^{1}H signals for that species and to look for long-range correlations and coupling to other monosaccharide species. HSQC and ^{13}C spectra were used continuously to assign the ^{13}C signals that correlated with the specific ^{1}H signals. The different samples were usually compared to each other using overlay plots, for example overlaying the HSQC spectra from IOE-WN and IOI-WAcF1 to look for differences. If some signals could still not be assigned, either due to overlap with other signals or because of weak signal intensity, CASPER prediction was used to get an idea of the location (Jansson et al., 2006; Lundborg & Widmalm, 2011). In general it was difficult to find evidence of linkages between the different monomers in the HMBC and NOESY spectra, such as direct linkages from Xyl to Glc, or from GalA to Gal. Since all fractions were highly heterogeneous, it means that either these linkage signals were too weak to observe by NMR analysis, or that the fractions consisted of several separate polymers which were diluted together during fractionation. However, the latter explanation seems unlikely. During column chromatography, we loaded sample onto the column step-wise, a small amount

each time, and monitored the fractionation using the phenol-sulfuric acid assay. The polysaccharides were eluted at the same point each time, and if the samples were to be a mix of "entangled" polymers, there would have been variation in elution times from experiment to experiment. It therefore seems more likely that the fractions contained heteropolysaccharides but that the linkages were too difficult to capture by NMR spectroscopy due to low relative abundance of each specific linkage signal. All water-soluble samples had presence of major peaks in the anomeric region, defined as having chemical shift values between 4.5-5.5 ppm for ^{1}H and 95-105 ppm for ^{13}C (Fig. 3) (Duus et al., 2000). Typically, α-anomeric signals will appear downfield of β-anomeric signals for ^{1}H chemical shifts, and opposite for ^{13}C chemical shifts. The chemical shift values of the major signals found are presented in Table 4. There was evidence of reducing ends present in some fractions (Fig. S9-S14). Although these signals correlated with the relative sizes of the fractions (lower M_w means more reducing ends), the signals were stronger than they should be according to SEC-MALLS. For example, in IOI-WAcF2 the total signal strength of the reducing ends was about 6.7% compared to the anomeric signals, theoretically giving a M_w of ~2.5 kDa instead of 14 kDa as seen from SEC-MALLS (Table 1). One possible explanation for the observed effect is that reducing ends located near the surface would give stronger NMR signals than the monomers located inside the polymer, since they would be more flexible. This could be particularly true for the polysaccharides in this study, since the R_G values suggest that the structures are very compact (Table 1). This could result in the reducing ends having T2 relaxation times more similar to oligo- or monosaccharides, and longer T2 relaxation times would in turn result in lower loss of magnetization during mixing times (Duus et al., 2000).

Table 4: Chemical shift values of the major signals found in the water-extracted polysaccharide fractions from *I. obliquus*. The values are expressed as ppm from each position in that species, from C1/H1 (1) to C6/H6 (6), and are based mainly on spectra from IOE-WN, IOI-WAc and IOI-WAcF1-F3. Some of the species could only be partially assigned due to overlaps and/or weak signal intensities.

Type of monosaccharide w/linkage	1	2	3	4	5	6	3-*O*-Me
(1→3)-β-Glc-(1→3)							
δ^{13}C	102.48	73.17	84.59	68.17	75.44	60.80	
δ^{1}H	4.87	3.65	3.85	3.61	3.6	3.83/4.03	
1→6)-β-Glc-(1→3)							
δ^{13}C	102.92	73.35	75.42	69.62	74.59	68.85	
δ^{1}H	4.80	3.47	3.62	3.51	3.80	3.96/4.31	
(1→6)-β-Glc-(1→6)							
δ^{13}C	102.72	73.05	75.62	69.52	74.82	68.85	
δ^{1}H	4.61	3.42	3.59	3.55	3.72	3.96/4.31	

	C1/H1	C2/H2	C3/H3	C4/H4	C5/H5	C6/H6	
(1→3)-β-Glc-(1→6)							
$\delta^{13}C$	102.40	72.58	84.79	68.11	75.44	60.80	
δ^1H	4.63	3.61	3.84	3.60	3.58	3.83/4.03	
T-β-Glc-(1→6)							
$\delta^{13}C$	102.72	73.05	75.62	69.52	74.82	60.80	
δ^1H	4.61	3.42	3.59	3.55	3.72	3.83/4.03	
(1→4)-β-Xyl							
$\delta^{13}C$	101.87	74.21			62.9		
δ^1H	4.55	3.34	3.66	3.82	3.46/4.18		
T-β-Xyl-(1→4)							
$\delta^{13}C$	101.69				65.16		
δ^1H	4.56	3.38			3.4/4.06		
(1→6)-α-Gal-(1→6)							
$\delta^{13}C$	97.72	67.95	69.83	69.23	69.11	66.76	
δ^1H	5.08	3.93	3.97	4.11	4.26	3.78/4.01	
(1→6)-α-3-O-Me-Gal-(1→6)							
$\delta^{13}C$	97.72	67.42	78.77	65.1	68.77	66.76	56.02
δ^1H	5.07	3.97	3.63	4.38	4.27	3.78/4.01	3.53
(1→4)-α-GalA-(1→4)							
$\delta^{13}C$	98.92	68.02	68.62	77.72	71.12	174.70	
δ^1H	5.17	3.85	4.09	4.52	4.85		
(1→3)-α-Man							
$\delta^{13}C$	102.1	70.38	78.43			62.84	
δ^1H	5.21	3.86	4.12			3.82/3.98	
(1→4)-α-GlcA							
$\delta^{13}C$	98.9						
δ^1H	5.34		4.21				
(1→2)-α-Rha							
$\delta^{13}C$	102.3					16.93	
δ^1H	5.09	4.18		3.5	3.9	1.33	

19

3.8.1 β-glucose

The HSQC spectra revealed the presence of two main signal clusters in the β-anomeric region located at (^{1}H/^{13}C) ~4.85/102.5 ppm and ~4.62/102.9 ppm (Fig. 3). With the use of DQF-COSY, TOCSY as well as HSQC-TOCSY spectra, the signals were suggested to come from β-glucose: β-Glc-(1→3)-species at ~4.85/103 ppm and β-Glc-(1→6) species at ~4.6/103 ppm (Table 4). The peaks were too broad to contain just one signal, and the HSQC and ^{13}C spectra indicated presence of signals from several different anomeric carbons, probably variations of the different β-Glc species, such as (1→3-β-Glc-1→3), (1→6-β-Glc-1→3), (1→3-β-Glc-1→6), and (1→6-β-Glc-1→6). Anomeric signals from even more complex species including (1→3, 6)-branching points, or with C2 in glucose additionally substituted by another monosaccharide as suggested from the linkage analysis data (Table 3) would also be located in the same anomeric signal clusters. Further, signals from terminal glucose would also be located here, as these could be defined as pure β-Glc-(1→3) or β-Glc-(1→6) species with no other substitutions. The two main clusters were defined on the basis of the assignment methods described above, and also because the two groups could be differentiated by the relatively large difference in shift values for C6 in the HSQC spectra, where the (1→6)-β-Glc has a ^{13}C chemical shift downfield of its (1→3)-β-Glc counterpart (Table 4). In addition, the C3 signal from (1→3)-β-Glc has a very characteristic chemical shift value, in our samples observed at ~3.85/85 ppm in the HSQC spectra, thus confirming that the signals come from glucose. It was attempted to find correlations between the various β-Glc species by comparing integrals in the HSQC spectra (which could not be done in 1D spectra due to overlaps). Although 2D integrals are less accurate and overlap also occurred in these spectra, some clues were found that could indicate a possible configuration. In IOE-WN, the HSQC integral from the anomeric β-Glc-(1→3) cluster was approximately the same size as the signal from C3/H3 in (1→3)-β-Glc. The signal from C4/H4 in (1→3)-β-Glc was about 25 % smaller than the others, but a signal located at same ^{13}C ppm but 0.1 ^{1}H ppm downfield corresponded well with these 25 % and according to CASPER this signal could come from (1→3, 6)-β-Glc-(1→), suggesting several branching points in the polymer. The relative proportion of (1→3)-linked and (1→6)-linked β-Glc was approx. 1:1 for most samples according to GC-MS (Table 3), while the signal cluster in the HSQC spectra from β-Glc-(1→6)-species was twice as big as the β-Glc-(1→3)-cluster (Fig. 3). Methylation/GC-MS analysis does not give information on how terminal residues are linked but NMR does, and a possible explanation for the difference in signal strength could therefore be that most of the terminal Glc in our samples is (1→6)-linked.

3.8.2 β-xylose

Some signals close to the two major peaks in the β-anomeric region were assigned to (1→4)-linked β-xylose species (Fig. 3, Table 4). β-Xyl has axial protons for H1, H2, H3 and H4, making it easier to detect than some other monosaccharides since the H,H couplings will give strong signals which can be correlated through DQF-COSY and TOCSY. The anomeric ^{1}H signals

could therefore be correlated throughout the molecule from H1-H5, but some of the ^{13}C signals could not be assigned due to overlaps (C3 and C4). In the HSQC spectra, opposite phase chemical shifts for H5a and H5b were in accordance with CASPER prediction for (1→4)-β-Xyl and terminal β-Xyl(1→4). The H-H split of C5 in xylose is quite large and characteristic compared to some other monosaccharides (Agrawal, 1992). There were some differences between the samples for the H5 signals. For example, IOE-WN had one clear [1]H-[1]H-split from H5 in (1→4)-β-Xyl, while in IOI-WN there were two such splits differing by 0.05 ppm, suggesting more than one (1→4)-β-Xyl species in IOI-WN. This could mean that xylose chains of various lengths or xylose being in different local environments are present, giving rise to more signals. From GC-MS data it was found that the IOE-WN fraction had slightly more T-Xyl (4.7 %) than (1→4)-Xyl (4.2 %), suggesting that xylose is substituting a main polysaccharide chain as either mono- or disaccharides with (1→4) linkages. The IOI-WN fraction had slightly more (1→4)-Xyl (3.8 %) than T-Xyl (3.1 %), suggesting that the xylose side chains would be of varying lengths, which would fit well with the NMR spectra observed. However, we could not observe any HMBC correlations from xylose to glucose or galactose, but this could also be due to the relative rarity of these linkages in the samples. As seen from Table 2, xylose is present in relatively high amounts in all fractions, also when galactose, mannose and galacturonic acid levels are low. It therefore seems likely that xylose is somehow linked to glucose within the polymers chain.

3.8.3 α-galactose and α-3-O-Me-Gal

All samples had presence of several strong signals in the α-anomeric region (Fig. 3). The signal at 5.07/97.72 ppm was suggested to come from (1→6)-α-3-O-Me-Gal. Using DQF-COSY it was found that this signal actually correlated with two separate H2 signals, at 3.97 and 3.93 ppm. Using DQF-COSY and TOCSY the signals at 3.97 ppm could be assigned through the spin system from H2-H6. The HMBC spectrum showed a correlation between the H3/C3 of this species to a methyl peak at 3.53/56.02 ppm, and as such this species was designated (1→6)-α-3-O-Me-Gal. The other signal in the same anomeric peak was assigned to (1→6)-α-Gal. According to CASPER prediction, the anomeric ^{13}C chemical shift values from these two species should actually be separated by 2 ppm. However, since the signal cluster ranged from ~96.80-99 ppm, and others also have reported the same findings as us, it seems logical that the two signals would be located in the same area (Smiderle et al., 2008). This would also explain the relatively strong intensity of the anomeric peak, which had equal signal intensity as the β-Glc-(1→6) signal cluster. In both species the rest of the ^{13}C signals could be assigned using HSQC and HMBC. The ^{13}C signal from C6 could not be differentiated between the two species, and had a relatively downfield shift value compared to the expected value for galactose (Agrawal, 1992). This was probably due to the substitution at C6 with another Gal residue, which was further strengthened by finding a strong correlation from C1 to C6 in HMBC as well, suggesting that a part of the

polymer chain has a (1→6)-α-Gal-(1→6) motif with about every second or third residue being 3-*O*-methylated.

3.8.4 α-GalA

In the acidic fractions only, a signal at 5.17/98.92 ppm with strong intensity was found in the α-anomeric region (Fig. 3a, Fig S9-S14). The signal was suggested to come from (1→4)-α-GalA since this species should be present in high amounts in acidic fractions and absent from the neutral fractions according to GC-MS data (Table 3). The signal could be correlated throughout the ^{1}H spin system from H1-H5 and it was also possible to assign the ^{13}C signals to each ^{1}H signal (Table 4). According to CASPER prediction, GalA was expected to have ^{1}H chemical shifts values for H4 and H5 close to the β-anomeric region but with highly different ^{13}C values, and this seemed to be the case in our samples as well, with H4 at 4.52 ppm and H5 at 4.85 ppm (Agrawal, 1992). These two signals could be used to distinguish GalA from GlcA, since GlcA would have ^{1}H shift values at much lower ppm according to CASPER. In the ^{13}C and HMBC spectra there was a signal at 174.70 ppm which indicated presence of a C6 carboxyl group coming from an uronic acid. Further, in several HMBC spectra we could correlate C4 and H1 and H4 and C1 to each other by HMBC, indicating that this species was a long chain of (1→4)-α-GalA-(1→4). No linkage correlations between GalA and other species could be observed, but this could be due to a very low relative abundance of monomers linking the GalA chain to the rest of the polymer.

3.8.5. Other α-linked species

In most fractions there were also several minor signals that could not be completely assigned to specific species due to signal overlap and the relative weakness of the signals (Figure 3a). GC and GC-MS data indicated that glucuronic acid, rhamnose and mannose were present in various amounts in all samples (Table 3) and several of the signals in the α-anomeric region probably came from these monosaccharides. As for GlcA it was difficult to locate most signals, probably because of the low abundance in all samples (Table 4). According to CASPER prediction, (1→4)-α-GlcA is expected to have anomeric ^{1}H chemical shift values downfield of GalA, and the anomeric signal at 5.33/98.62 was consistently present in the acidic fractions where (1→4)-GlcA was present. Although clear correlations to other signals could not be seen using DQF-COSY, the anomeric signal could be correlated to a ^{1}H signal at 4.21 ppm using the TOCSY spectrum, which could be from H3 in the same spin system, and this also was in relative accordance with CASPER prediction. Other signals from (1→4)-GlcA could not be observed due to unknown reasons, thus the signal assignments remains unclear. GC-MS data also indicated the presence of (1→2)- and (1→3)-linked mannose, and mannose is usually in the α-configuration in fungi (Arana et al., 2009). The HSQC signal at 5.21/102.27 ppm could come from (1→3)-linked α-Man (Fig. 3). However, this signal could not be correlated further to the

22

H2 signal, which could be due to the fact that mannose can be quite difficult to deduce by NMR spectroscopy, as the equatorial H2 gives weak couplings to H1 and H3. This means that high amounts of each mannose species probably would be required for sufficient signal intensities to be produced. The absence of clear correlations is in this sense in accordance with GS-MS data which suggested that only small amounts of each mannose species were present in the samples (Table 3). Additionally, it was only in IOI-WAcF2 – the fraction with the highest amount of (1→3)-α-Man - that the anomeric signal could be located clearly, with some traces in the IOI-WAc sample as well. There was also a slight indication of a correlation between [1]H-signals at 4.155 and 5.369 ppm in NOESY, which could come from mannose (Fig. S15). However, this could not be found in HSQC-TOCSY or other spectra, which makes it possible that it could come from across the glycosidic linkage and not from the same monomer.

Rhamnose was thought to be in α-configuration due to the presence of several non-assigned anomeric signals in the α-anomeric region. Using spectra from IOI-WAcF3, a signal was located at 1.33/16.93 ppm in HSQC which likely was from a methyl in a 6-deoxy sugar. In DQF-COSY, this signal had correlations to another ^{1}H signal at ~3.90 ppm, which could be the H5 signal from α-rhamnose (Agrawal, 1992). This signal could be correlated to signals at ~3.5 ppm and 4.18 ppm using TOCSY, and although the peaks were quite broad this suggests the presence of at least one α-Rha species in the samples, probably (1→2)-α-Rha (Fig. S16 and S17).

3.8.6 IOI-A1

The alkali-extracted fraction IOI-A1 was also subjected to NMR analysis. However, since the fraction was dissolvable only in alkali and neither H_2O or dimethyl sulfoxide (DMSO), the sample was dissolved in 0.1 M NaOH in D_2O which led to some results not consistent with the other samples. The HSQC spectrum revealed presence of some strong signals coming from β-Glc species (Fig. S18). Some of the signals could be assigned with a high degree of certainty, such as two (1→3)-β-Glc signals at 3.79/87.7 ppm (from H3/C3) and 3.83/4.02/61.1 ppm (from H6a/H6b/C6). Other signals seemed to come from (1→6)-linked species. Some of the signals had shifted notably compared to the other samples, possibly due to the difference in pH. In addition, the large size of the IOI-A1 fraction (>450 kDa) and the presence of Na^+ in the sample could give weaker signals than expected, especially for the backbone of the polymer which is primarily made up of (1→3)-linked β-Glc, whereas the side-chains of higher mobility would be less affected.

The GC-MS data suggested that IOI-A1 contained mainly (1→3)-Glc (57.3 %), with presence of (1→6)-Glc (3.3 %), (1→3, 6)-Glc (5.6 %) and T-Glc (8 %) (Table 3). The strongest signals seen in [13]C (Fig. S31) and HSQC spectra of IOI-A1 came from what seemed to be either (1→6)-linked β-Glc or (1→3, 6)-β-Glc species, and it therefore seems likely that the terminal β-Glc would be (1→6)-linked, thus accounting for some of the signals seen in the NMR spectra. This would give a polymer with a backbone consisting of (1→3)-linked β-Glc with short side chains of (1→6)-linked β-Glc, possibly substituted with β-Xyl in between.
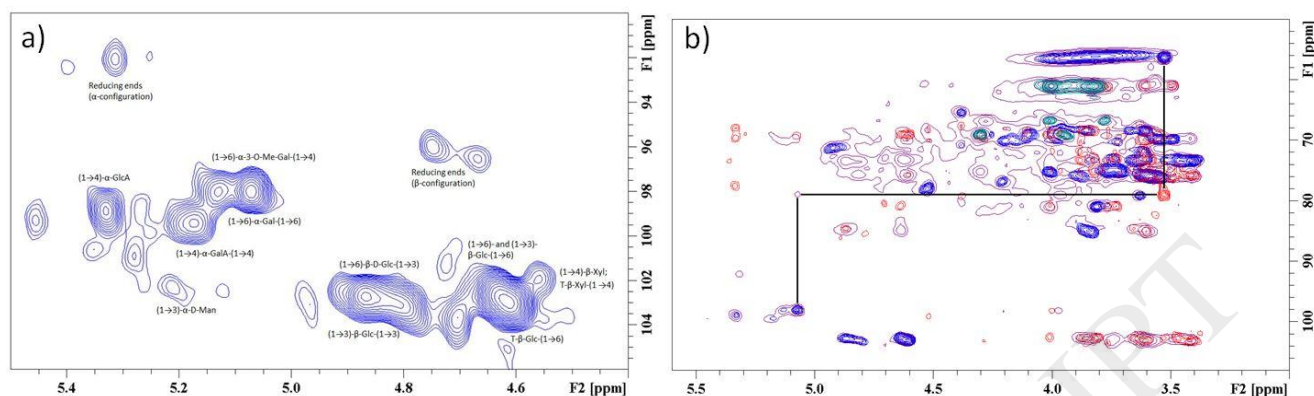
23

Fig. 3: (a) NMR analysis of fraction IOI-WAcF2, showing the anomeric region from the HSQC spectrum with assignments of the major signals in this region. Chemical shifts are expressed in ppm. (b) Overlay plot from IOI-WAcF2 of HSQC (blue)/HSQC-TOCSY (purple)/HMBC (red), showing the main carbohydrate region between 3-6 ppm/50-110 ppm ^{1}H/^{13}C. This plot gives an idea of the complexity of the sample. The black line shows a direct link from the *O*-methyl signal at 3.53/56.02 ppm to a C3 signal from α-Gal at 3.63/78.77 ppm, which could be traced back to the C1 signal at 5.07/97.72 ppm. This species was assigned as (1→6)-3-*O*-Me-α-Gal.

3.9 Periodate oxidation and Smith degradation

IOE-WN was subjected to periodate oxidation and Smith degradation to find clues about the relationship between homologous stretches in the polymer chain and linkages. Since the (1→3) linked sugars should not be hydrolyzed by the weak acid utilized after periodate oxidation (0.05 M TFA), it would be expected that some oligosaccharides were produced if stretches of (1→3)-linked β-Glc existed (Kamerling & Gerwig, 2007). Fractionation of the degraded sample gave three main fractions which were analyzed by GC. While the two first fractions consisted of monomers (3-*O*-Me-Gal and Glc, respectively), the last fraction had a retention time in the middle of the maltotetraose and maltohexaose standards, and contained only glucose. This indicated that there were stretches of about 4-6 (1→3)-linked glucose monomers before a change in the polymer chain occurs. Given the relatively large proportion of (1→6) linked Glc and Gal in the samples, it could be that the main motif of the polysaccharides is (1→3)-linked β-Glc five monomers long with (1→6)-linked "kinks" in between with either Glc or Gal residues. There are some reports of similar structures in the literature, such as galactoglucans from the fungus *Lentinus fusipes* (Manna et al., 2017) and from the bacteria *Rhizobium meliloti* (Zevenhuizen, 1997). In addition, alternating (1→4)/(1→3)-linkages of glucose is the main motif in oat and barley β-glucans (Brennan & Cleary, 2005), suggesting that the possibility of alternating linkages in the main chain of polysaccharides from other species such as fungi may exist as well.

3.10 Nitric oxide (NO) assay

The polysaccharide fractions were screened for their ability to induce nitric oxide (NO) production in the murine dendritic cell line D2SC/1 and the murine macrophage cell line J774A1. NO regulates many processes in the immune system and is an important molecule in human physiology (Hickok & Thomas, 2010), and high NO production by macrophages and dendritic cells can be considered a marker for a pro-inflammatory phenotype (Curren Smith, 2015). To investigate the immunomodulating effect of *I. obliquus* polysaccharides, cells were incubated with polysaccharide fractions with or without IFN-γ for 24 h. IFN-γ has been shown to have a synergistic effect with TLR ligands on NO production in immune cells (Qiao et al., 2013; Totemeyer et al., 2006). The results are presented in Fig. 4. Although the fractions failed to activate NO production when used alone, most fractions demonstrated potent activity with IFN-γ at the highest concentration (100 μg/ml), indicating a synergistic effect which also was observed using the positive control Pam3CSK4. The neutral fraction IOE-WN gave a clear dose-response relationship, and was therefore considered the most promising fraction in this assay. IOE-WAc initially seemed promising; however it was found that this fraction contained LPS equivalent to 16 ng/ml at 100 μg/ml (0.16 %). The acidic fractions from the interior part contained polyphenolic traces which could influence the results. In preliminary experiments a phenolic fraction from *I. obliquus* had a repressive effect on NO production in J774.A1 cells pretreated with LPS and IFN-γ (data not shown), whereas others have found the same effect using polyphenolic extracts from various plants and fungi (Diaz, Jeong, Lee, Khoo, & Koyyalamudi, 2012). The absence of a clear dose-response relationship in the acidic fractions from the interior part (containing 4.2 - 9.7 % polyphenols) could therefore be due to the presence of polyphenols although it would not explain why the same fractions induced potent NO production at 100 μg/ml. The alkali-extracted IOI-A1 was not able to induce NO production in a dose-dependent manner, but demonstrated some activation even at the lowest concentration (1 μg/ml with IFN-γ) in the D2SC/1 cell line.
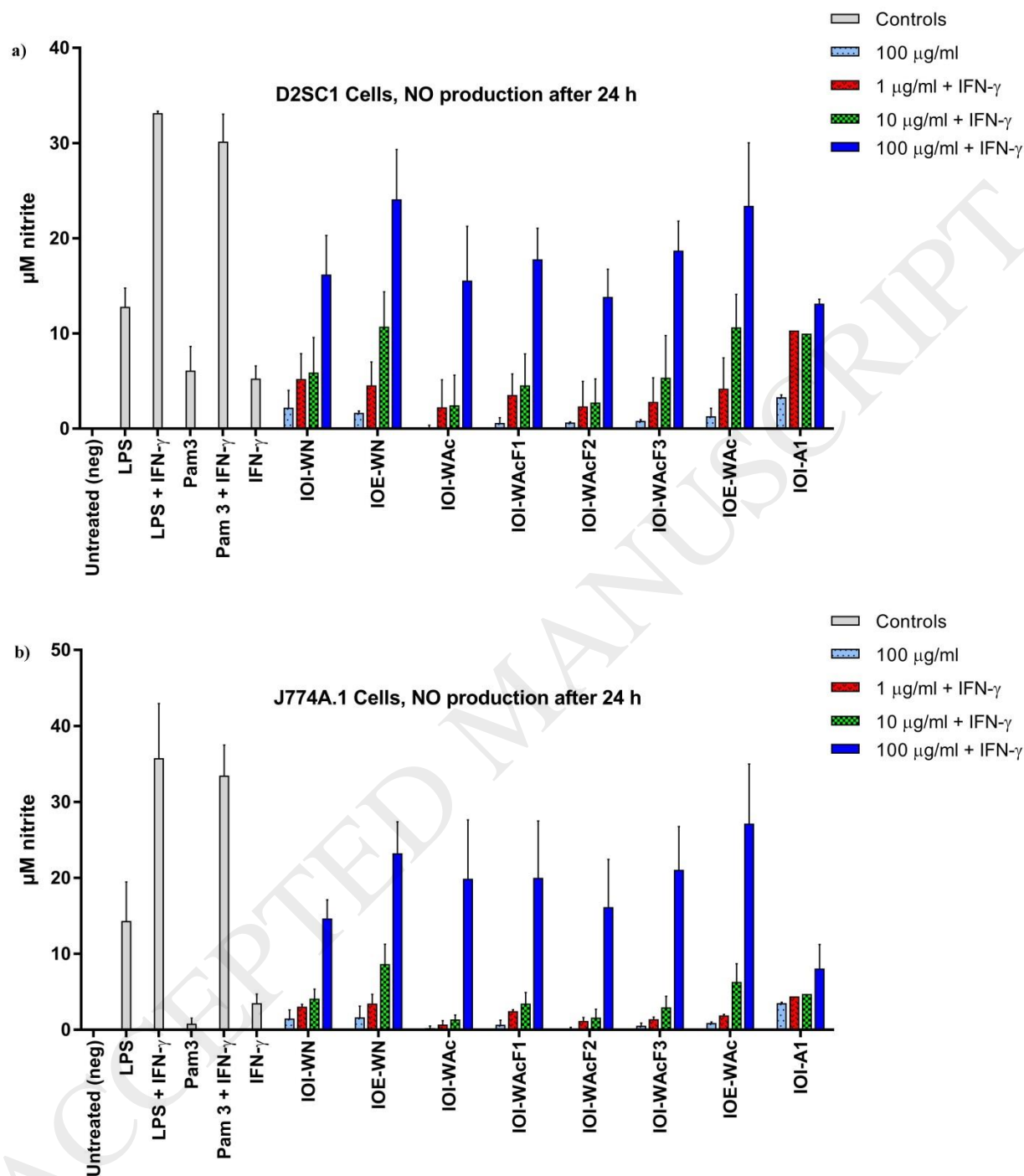
Fig. 4: NO production expressed as μM nitrite in the supernatant from D2SC/1 cells (a) and J774A.1 cells (b) after treatment with *I. obliquus* polysaccharide fractions with/without IFN-γ for 24 h. LPS (1 μg/ml), Pam3CSK4 (2 μg/ml) and IFN- γ (20 ng/ml) were used as positive controls alone and in combination. The untreated negative control had nitrite values ranging from 0.2-1 μM but this was set to zero for the presentation of the results.

3.11 Structure-function relationship

A clear structure-function relationship of the polysaccharides and their immunomodulating effects could not be established using the NO assay alone, but some suggestions were made. Since the neutral fractions seemed more active than the acidic ones, the GalA residues were probably not the most important for immune cell activation. Further, there was no obvious correlation between the amount of galactose and activity, since IOI-WAcF1 (~20% Gal/3-*O*-Me-Gal) and IOI-WAcF3 (~9% Gal/3-*O*-Me-Gal) gave similar results. Since the alkaline fraction IOI-A1 was not very active, it seems logical to conclude that soluble polysaccharides were better immune cell activators than particulate ones in this assay, in contrast with previous reports (Goodridge et al., 2011). However, the relative inactivity of IOI-A1 could also be due to its large size rather than solubility, or some other factors like the presence of xylose (14 %) in this fraction. The two neutral fractions IOI-WN and IOE-WN were very similar in terms of monosaccharide composition and types of linkages found, but IOE-WN seemed more promising in the NO assay. IOE-WN was slightly larger, having an M_w of 73 kDa vs. 60 kDa for IOI-WN. In addition, IOE-WN had a narrower weight-distribution according to SEC-MALLS which means a more homogenous polysaccharide fraction, and this could also explain some of the difference in activity. It seems likely that the (1→3)/(1→6)-β-Glc motif is, at least in part, responsible for the main effects observed in the experiments, but other factors such as three-dimensional shape could also be important. Fungal β-glucans of various kinds have previously been shown to be potent immune activators, and many different immune cell receptors have been associated with the recognition of such fungal structures (Erwig & Gow, 2016). Dectin-1 has for example been established as the main receptor for particulate (1→3)-β-glucans (Goodridge et al., 2011), but it could very well be that other receptors are involved in the recognition of soluble β-glucans such as the ones from *I. obliquus* described herein. One study found an increased production of TNF-α by RAW264.7 cells after treatment with a polysaccharide extract from *I. obliquus*, and this effect was sugggested to be via Toll-like receptor 2 (TLR2) interaction and not Dectin-1 or TLR-4 (Won et al., 2011). Although the effects in the mentioned study were measured indirectly, and the experiment was conducted using a crude polysaccharide extract obtained by ethanol precipiation only (probably containing substantial amount of melanin as well), the results encourage further testing of purified *I. obliquus* polysaccharides in similar assays.

4. Conclusion

To our knowledge, this study is the first comprehensive characterization of polysaccharides from the medicinal fungus *I. obliquus*. Water-extracted neutral and acidic polysaccharide fractions as well as an alkali-extracted polysaccharide fraction were isolated from the interior (IOI) and exterior (IOE) parts of *I. obliquus* sclerotia and characterized by chromatographic and spectroscopic methods. No major structural differences between fractions from IOI and IOE

were observed. The neutral polysaccharides IOI-WN (60 kDa) and IOE-WN (73 kDa) were heterogeneous and branched and consisted of a (1→3)-linked β-Glc backbone with (1→6)-linked kinks in the chain at approximately every fifth residue, with branches of (1→6)-linked β-Glc in addition to substantial amounts of (1→6)-linked α-Gal with 3-*O*-methylation at about every third Gal residue. The acidic polysaccharide fractions IOI-WAc, IOI-WAcF1, F2 and F3 and IOE-WAc (10-31 kDa) showed similar structural motifs as the neutral ones, differing mainly by the presence of (1→4)-linked α-GalA and α-GlcA. β-Xyl, α-Man and α-Rha were present in varying amounts in all fractions. The alkaline polysaccharide fraction IOI-A1 (>450 kDa) consisted mainly of (1→3)- and (1→6)-linked β-Glc and (1→4)-linked β-Xyl. GC-MS data from all fractions indicated that the polymer branching points were mainly found on β-Glc residues, thus these residues possibly connect the different parts of the polymers. However, such linkages could not be directly observed by NMR, and it should be attempted to clarify this in future studies. Several of the polysaccharide fractions showed promising results as immunomodulators as seen from the synergistic effect with IFN-γ on NO production in the murine cell lines J774.A1 and D2SC/1. The neutral polysaccharide fraction IOE-WN showed the most potent effect in the assay, increasing NO production at 10 µg/ml. It seems likely that the (1→3)/(1→6)-β-Glc motif within the polymer is important for bioactivity, but other factors such as three-dimensional shape could be equally important for the immunomodulating effect. The results presented herein encourage further exploration of the fine-structure, the structure-function relationship and bioactivity of polysaccharides from *I. obliquus.*

Appendix A. Supplementary data

Supplementary data associated with this article can be found in Appendix A in the online version.

References

Agrawal, K. A. (1992). NMR spectroscopy in the structural elucidation of oligosaccharides and glycosides. *Phytochemistry,* 31(10), 3307-3330.

Arana, D. M., Prieto, D., Roman, E., Nombela, C., Alonso-Monge, R., & Pla, J. (2009). The role of the cell wall in fungal pathogenesis. *Microbial Biotechnology,* 2(3), 308-320.

Austarheim, I., Christensen, B. E., Hegna, I. K., Petersen, B. O., Duus, J. O., Bye, R., . . . Paulsen, B. S. (2012). Chemical and biological characterization of pectin-like polysaccharides from the bark of the Malian medicinal tree Cola cordifolia. *Carbohydrate Polymers,* 89(1), 259-268.

Bouchard, A., Hofland, G. W., & Witkamp, G. J. (2007). Properties of Sugar, Polyol, and Polysaccharide Water-Ethanol Solutions. *Journal of Chemical & Engineering Data,* 52, 1838-1842.

Bradford, M. M. (1976). A Rapid and Sensitive Method for the Quantitation of Microgram Quantities of Protein Utilizing the Principle of Protein-Dye Binding. *Analytical Biochemistry,* 72, 248-254.

Brennan, C. S., & Cleary, L. J. (2005). The potential use of cereal (1→3,1→4)-β-d-glucans as functional food ingredients. *Journal of Cereal Science,* 42(1), 1-13.

Carbonero, E. R., Gracher, A. H., Rosa, M. C., Torri, G., Sassaki, G. L., Gorin, P. A., & Iacomini, M. (2008). Unusual partially 3-O-methylated alpha-galactan from mushrooms of the genus Pleurotus. *Phytochemistry,* 69(1), 252-257.

Cha, J. Y., Lee, S. Y., Lee, S. Y., & Chun, K. W. (2011). Basidiocarp formation by Inonotus obliquus on a living paper birch tree. *Forest Pathology,* 41(2), 163-164.

Chambers, R. E., & Clamp, J. R. (1971). An Assessment of Methanolysis and Other Factors Used in the Analysis of Carbohydrate-Containing Materials. *Biochemical Journal,* 125, 1009-1018.

Chen, Y., Huang, Y., Cui, Z., & Liu, J. (2015). Purification, characterization and biological activity of a novel polysaccharide from Inonotus obliquus. *International Journal of Biological Macromolecules,* 79, 587-594.

Curren Smith, E. W. (2015). Macrophage Polarization and Its Role in Cancer. *Journal of Clinical and Cellular Immunology,* 06(04).

de Santana-Filho, A. P., Noleto, G. R., Gorin, P. A. J., de Souza, L. M., Iacomini, M., & Sassaki, G. L. (2012). GC–MS detection and quantification of lipopolysaccharides in polysaccharides through 3-O-acetyl fatty acid methyl esters. *Carbohydrate Polymers,* 87(4), 2730-2734.

Diaz, P., Jeong, S. C., Lee, S., Khoo, C., & Koyyalamudi, S. R. (2012). Antioxidant and anti-inflammatory activities of selected medicinal plants and fungi containing phenolic and flavonoid compounds. *Chinese Medicine,* 7(26).

Du, B., Lin, C., Bian, Z., & Xu, B. (2015). An insight into anti-inflammatory effects of fungal beta-glucans. *Trends in Food Science & Technology,* 41(1), 49-59.

Dubois, M., Gilles, K. A., Hamilton, J. K., Rebers, P. A., & Smith, F. (1956). Colorimetric method for determination of sugars and related substances. *Analytical Chemistry,* 28, 350-356.

Duus, J. Ø., Gotfredsen, C. H., & Bock, K. (2000). Carbohydrate Structural Determination by NMR Spectroscopy: Modern Methods and Limitations. *Chemical Reviews,* 100, 4589-4614.

Eisenman, H. C., & Casadevall, A. (2012). Synthesis and assembly of fungal melanin. *Applied Microbiology and Biotechnology,* 93(3), 931-940.

Erwig, L. P., & Gow, N. A. (2016). Interactions of fungal pathogens with phagocytes. *Nature Reviews Microbiology,* 14(3), 163-176.

Fan, L., Ding, S., Ai, L., & Deng, K. (2012). Antitumor and immunomodulatory activity of water-soluble polysaccharide from Inonotus obliquus. *Carbohydrate Polymers,* 90(2), 870-874.

Fraser, I. P., Stuart, L., & Ezekowitz, R. A. (2004). TLR-independent pattern recognition receptors and anti-inflammatory mechanisms. *Journal of Endotoxin Research,* 10(2), 120-124.

Glamoclija, J., Ciric, A., Nikolic, M., Fernandes, A., Barros, L., Calhelha, R. C., . . . van Griensven, L. J. (2015). Chemical characterization and biological activity of Chaga (Inonotus obliquus), a medicinal "mushroom". *Journal of Ethnopharmacology, 162*, 323-332.

Goodridge, H. S., Reyes, C. N., Becker, C. A., Katsumoto, T. R., Ma, J., Wolf, A. J., . . . Underhill, D. M. (2011). Activation of the innate immune receptor Dectin-1 upon formation of a 'phagocytic synapse'. *Nature, 472*(7344), 471-475.

Hickok, J. R., & Thomas, D. D. (2010). Nitric Oxide and Cancer Therapy: The Emperor has NO Clothes. *Current Pharmaceutical Design, 16*(4), 381-391.

Hu, Y., Sheng, Y., Yu, M., Li, K., Ren, G., Xu, X., & Qu, J. (2016). Antioxidant activity of Inonotus obliquus polysaccharide and its amelioration for chronic pancreatitis in mice. *International Journal of Biological Macromolecules, 87*, 348-356.

Huang, S. Q., Li, J. W., Wang, Z., Pan, H. X., Chen, J. X., & Ning, Z. X. (2010). Optimization of alkaline extraction of polysaccharides from Ganoderma lucidum and their effect on immune function in mice. *Molecules, 15*(5), 3694-3708.

Hwang, B. S., Lee, I. K., & Yun, B. S. (2016). Phenolic compounds from the fungus Inonotus obliquus and their antioxidant properties. *The Journal of Antibiotics, 69*(2), 108-110.

I., C., & Kerek, F. (1984). A simple and rapid method for the permethylation of carbohydrates. *Carbohydrate Research, 131*, 209-217.

Ina, K., Kataoka, T., & Ando, T. (2013). The Use of Lentinan for Treating Gastric Cancer. *Anti-Cancer Agents in Medicinal Chemistry, 13*, 681-688.

Jansson, P. E., Stenutz, R., & Widmalm, G. (2006). Sequence determination of oligosaccharides and regular polysaccharides using NMR spectroscopy and a novel Web-based version of the computer program CASPER. *Carbohydrate Research, 341*(8), 1003-1010.

Kamerling, J. P., & Gerwig, G. J. (2007). *Strategies for the Structural Analysis of Carbohydrates*: Elsevier Ltd.

Kapoor, S. (2014). Lentinan: clinical benefit in the management of systemic malignancies. *Surgery Today, 44*(7), 1389.

Kim, Y. O., Han, S. B., Lee, H. W., Ahn, H. J., Yoon, Y. D., Jung, J. K., . . . Shin, C. S. (2005). Immuno-stimulating effect of the endo-polysaccharide produced by submerged culture of Inonotus obliquus. *Life Sciences, 77*(19), 2438-2456.

Kim, Y. O., Park, H. W., Kim, J. H., Lee, J. Y., Moon, S. H., & Shin, C. S. (2006). Anti-cancer effect and structural characterization of endo-polysaccharide from cultivated mycelia of Inonotus obliquus. *Life Sciences, 79*(1), 72-80.

Kukulyanskaya, T. A., Kurchenko, N. V., Kurchenko, V. P., & Babitskaya, V. G. (2002). Physicochemical Properties of Melanins Produced by the Sterile Form of Inonotus obliquus ("Chagi") in Natural and Cultivated Fungus. *Applied Biochemistry and Microbiology, 38*(1), 58-61.

Lee, K. R., Lee, J. S., Song, J. E., Ha, S. J., & Hong, E. K. (2014). Inonotus obliquus-derived polysaccharide inhibits the migration and invasion of human non-small cell lung carcinoma cells via suppression of MMP-2 and MMP-9. *International Journal of Oncology, 45*(6), 2533-2540.

Lieder, R., Petersen, P. H., & Sigurjonsson, O. E. (2013). Endotoxins-the invisible companion in biomaterials research. *Tissue Engineering Part B: Reviews, 19*(5), 391-402.

Liu, J., Willför, S., & Xu, C. (2015). A review of bioactive plant polysaccharides: Biological activities, functionalization, and biomedical applications. *Bioactive Carbohydrates and Dietary Fibre, 5*(1), 31-61.

Lu, C. C., Hsu, Y. J., Chang, C. J., Lin, C. S., Martel, J., Ojcius, D. M., . . . Young, J. D. (2016). Immunomodulatory properties of medicinal mushrooms: differential effects of water and ethanol extracts on NK cell-mediated cytotoxicity. *Innate Immunity, 22*(7), 522-533.

Lundborg, M., & Widmalm, G. (2011). Structural analysis of glycans by NMR chemical shift prediction. *Analytical Chemistry,* 83(5), 1514-1517.

Ma, L., Chen, H., Dong, P., & Lu, X. (2013). Anti-inflammatory and anticancer activities of extracts and compounds from the mushroom Inonotus obliquus. *Food Chemistry,* 139(1-4), 503-508.

Manna, D. K., Maity, P., Nandi, A. K., Pattanayak, M., Panda, B. C., Mandal, A. K., . . . Islam, S. S. (2017). Structural elucidation and immunostimulating property of a novel polysaccharide extracted from an edible mushroom Lentinus fusipes. *Carbohydrate Polymers,* 157, 1657-1665.

Min-Woong, L., Hyeon-Hur, Kwang-Choon, C., Tae-Soo, L., Kang-Hyeon, K., & Jankovsky, L. (2008). Introduction to Distribution and Ecology of Sterile Conks of Inonotus obliquus. *Mycobiology,* 36(4), 199-202.

Nyman, A. A., Aachmann, F. L., Rise, F., Ballance, S., & Samuelsen, A. B. (2016). Structural characterization of a branched (1-->6)-alpha-mannan and beta-glucans isolated from the fruiting bodies of Cantharellus cibarius. *Carbohydrate Polymers,* 146, 197-207.

Pettolino, F. A., Walsh, C., Fincher, G. B., & Bacic, A. (2012). Determining the polysaccharide composition of plant cell walls. *Nature Protocols,* 7(9), 1590-1607.

Prados-Rosales, R., Toriola, S., Nakouzi, A., Chatterjee, S., Stark, R., Gerfen, G., . . . Casadevall, A. (2015). Structural Characterization of Melanin Pigments from Commercial Preparations of the Edible Mushroom Auricularia auricula. *Journal of Agricultural and Food Chemistry,* 63(33), 7326-7332.

Qiao, Y., Giannopoulou, E. G., Chan, C. H., Park, S. H., Gong, S., Chen, J., . . . Ivashkiv, L. B. (2013). Synergistic activation of inflammatory cytokine genes by interferon-gamma-induced chromatin remodeling and toll-like receptor signaling. *Immunity,* 39(3), 454-469.

Rhee, S. J., Cho, S. Y., Kim, K. M., Cha, D.-S., & Park, H.-J. (2008). A comparative study of analytical methods for alkali-soluble β-glucan in medicinal mushroom, Chaga (Inonotus obliquus). *LWT-Food Science and Technology,* 41(3), 545-549.

Saar, M. (1991). Fungi in Khanty Folk Medicine. *Journal of Ethnopharmacology*, 175-179.

Schwartz, B., & Hadar, Y. (2014). Possible mechanisms of action of mushroom-derived glucans on inflammatory bowel disease and associated cancer. *Annals of Translational Medicine,* 2(2), 19.

Shashkina, M. Y., Shashkin, P. N., & Sergeev, A. V. (2006). Chemical and medicobiological properties of chaga (review). *Pharmaceutical Chemistry Journal,* 40(10), 560-568.

Shikov, A. N., Pozharitskaya, O. N., Makarov, V. G., Wagner, H., Verpoorte, R., & Heinrich, M. (2014). Medicinal plants of the Russian Pharmacopoeia; their history and applications. *Journal of Ethnopharmacology,* 154(3), 481-536.

Smiderle, F. R., Olsen, L. M., Carbonero, E. R., Marcon, R., Baggio, C. H., Freitas, C. S., . . . Iacomini, M. (2008). A 3-O-methylated mannogalactan from Pleurotus pulmonarius: structure and antinociceptive effect. *Phytochemistry,* 69(15), 2731-2736.

Staudacher, E. (2012). Methylation – an uncommon modification of glycans. *The Journal of Biological Chemistry,* 393(8), 675-685.

Swain, T., & Hillis, W. E. (1959). The phenolic constituents of Prunus domestica. I. - The quantitative analysis of phenolic constituents. *Journal of the Science of Food and Agriculture,* 10(1), 63-68.

Totemeyer, S., Sheppard, M., Lloyd, A., Roper, D., Dowson, C., Underhill, D., . . . Bryant, C. (2006). IFN-γ Enhances Production of Nitric Oxide from Macrophages via a Mechanism That Depends on Nucleotide Oligomerization Domain-2. *The Journal of Immunology,* 176(8), 4804-4810.

Wei, S., & Van Griensven, L. J. (2008). Pro- and Antioxidative Properties of Medicinal Mushroom Extracts. *International Journal of Medicinal Mushrooms,* 10(4), 315-324.

Whistler, R. L., & Wolfrom, M. L. (1963). *Reactions of Carbohydrates*. **New York**: Academic Press Inc.

Wiercigroch, E., Szafraniec, E., Czamara, K., Pacia, M. Z., Majzner, K., Kochan, K., . . . Malek, K. (2017). Raman and infrared spectroscopy of carbohydrates: A review. *Spectrochimica Acta Part A: Molecular and Biomolecular Spectroscopy,* 185, 317-335.

Won, D. P., Lee, J. S., Kwon, D. S., Lee, K. E., Shin, W. C., & Hong, E. K. (2011). Immunostimulating activity by polysaccharides isolated from fruiting body of Inonotus obliquus. *Molecules and Cells,* 31(2), 165-173.

Xu, X., Quan, L., & Shen, M. (2015). Effect of chemicals on production, composition and antioxidant activity of polysaccharides of Inonotus obliquus. *International Journal of Biological Macromolecules,* 77, 143-150.

Yang, Y., Zhang, J., Liu, Y., Tang, Q., Zhao, Z., & Xia, W. (2007). Structural elucidation of a 3-O-methyl-D-galactose-containing neutral polysaccharide from the fruiting bodies of Phellinus igniarius. *Carbohydrate Research,* 342(8), 1063-1070.

Yapo, B. M. (2011). Pectic substances: From simple pectic polysaccharides to complex pectins—A new hypothetical model. *Carbohydrate Polymers,* 86(2), 373-385.

Youn, M. J., Kim, J. K., Park, S. Y., Kim, Y., Park, C., Kim, E. S., . . . Park, R. (2009). Potential anticancer properties of the water extract of Inonotus obliquus by induction of apoptosis in melanoma B16-F10 cells. *Journal of Ethnopharmacology,* 121(2), 221-228.

Zevenhuizen, L. P. T. M. (1997). Succinoglycan and galactoglucan. *Carbohydrate Polymers,* 33, 139-144.

Zhang, M., Cui, S. W., Cheung, P. C. K., & Wang, Q. (2007). Antitumor polysaccharides from mushrooms: a review on their isolation process, structural characteristics and antitumor activity. *Trends in Food Science & Technology,* 18(1), 4-19.

Zhao, F., Mai, Q., Ma, J., Xu, M., Wang, X., Cui, T., . . . Han, G. (2015). Triterpenoids from Inonotus obliquus and their antitumor activities. *Fitoterapia,* 101, 34-40.

Zheng, W., Miao, K., Liu, Y., Zhao, Y., Zhang, M., Pan, S., & Dai, Y. (2010). Chemical diversity of biologically active metabolites in the sclerotia of Inonotus obliquus and submerged culture strategies for up-regulating their production. *Applied Microbiology and Biotechnology,* 87(4), 1237-1254.